

Metabolic Aggressiveness in Benign Meningiomas with Chromosomal Instabilities

Daniel Monleón¹, José Manuel Morales², Ana Gonzalez-Segura³, José Manuel Gonzalez-Darder⁴, Rosario Gil-Benso³, Miguel Cerdá-Nicolás^{3,5}, and Concepción López-Ginés³

Abstract

Meningiomas are often considered benign tumors curable by surgery, but most recurrent meningiomas correspond to histologic benign tumors. Because alterations in chromosome 14 among others have suggested clinical aggressiveness and recurrence, determining both the molecular phenotype and the genetic profile may help distinguish tumors with aggressive metabolism. The aim of this study was to achieve higher specificity in the detection of meningioma subgroups by measuring chromosomal instabilities by fluorescence *in situ* hybridization and cytogenetics and metabolic phenotypes by high-resolution magic angle spinning spectroscopy. We studied 46 meningioma biopsies with these methodologies. Of these, 34 were of WHO grade 1 and 12 were of WHO grade 2. Genetic analysis showed a subgroup of histologic benign meningioma with chromosomal instabilities. The metabolic phenotype of this subgroup indicated an aggressive metabolism resembling that observed for atypical meningioma. According to the metabolic profiles, these tumors had increased energy demand, higher hypoxic conditions, increased membrane turnover and cell proliferation, and possibly increased resistance to apoptosis. Taken together, our results identify distinct metabolic phenotypes for otherwise benign meningiomas based on cytogenetic studies and global metabolic profiles of intact tumors. Measuring the metabolic phenotype of meningioma intact biopsies at the same time as histopathologic analysis may allow the early detection of clinically aggressive tumors. *Cancer Res*; 70(21); 8426–34. ©2010 AACR.

Introduction

Meningiomas are often considered benign tumors curable by surgery. However, ~20% of meningiomas with histologic low grade may be clinically aggressive and recur (1). Meningiomas are neoplasms that arise from the leptomeningeal covering of the brain and spinal cord, accounting for 15% to 20% of all central nervous system tumors. The current standards for diagnosis of meningiomas are clinical and pathologic findings. The WHO classifies meningiomas into three histologic grades: grade 1 (benign), grade 2 (atypical), and grade 3 (anaplastic), in accordance with the clinical prognosis (2). Signs of malignancy in meningioma include marked vascularity, loss of organoid structure, mitotic figures, nuclear pleomorphism, prominent nucleoli, focal necrosis, or infiltration to the adjacent brain. Atypical and anaplastic meningiomas show a high index of recurrence

5 years after complete resection and are associated with lower survival rates compared with benign meningiomas (3). However, in absolute numbers, most recurrent meningiomas correspond to histologic benign tumors. The potential aggressiveness of an individual meningioma is still difficult to evaluate.

The genesis of meningiomas has been associated with loss of genetic material on chromosome 22. Monosomy of this chromosome is the most common genetic alteration in meningioma and was one of the first cytogenetic alterations described in solid tumors (4, 5). Loss of 1p and alterations in chromosome 14 are present in many atypical meningioma (6). Losses in 6q, 10, and 18q and gains on 1q, 9q, 12q, 15q, 17q, and 20q are also common in atypical meningioma (7). Based on this information, genetic characterization of meningiomas has some value in the subclassification of meningiomas. Recent studies show that benign tumors with alterations in chromosome 14 among others may be clinically aggressive and recur (8). However, correlations between a genetic profile and a clinical phenotype, which typically takes time to develop, are affected by many different variables. On the other hand, little is known about the effect of these chromosomal instabilities on the metabolic phenotype of the tumor. The determination of the molecular phenotype simultaneously to the genetic profile may help in further distinguishing metabolically aggressive tumors. This distinction may also aid in determining the aggressiveness of surgical resection and the necessity of combined radiation therapy. Additional criteria for better classification of meningiomas

Authors' Affiliations: ¹Fundación de Investigación del Hospital Clínico Universitario de Valencia/INCLIVA; ²Unidad Central de Investigación en Medicina and ³Departamento de Patología, Universitat de Valencia; ⁴Servicio de Neurocirugía, Hospital Clínico Universitario de Valencia, Valencia, Spain; and ⁵Centro de Investigación Biomédica en Red de Enfermedades Respiratorias, Madrid, Spain

Corresponding Author: Daniel Monleón, Fundación de Investigación del Hospital Clínico Universitario de Valencia, Avda. Blasco Ibáñez, 17, Valencia 46010, Spain. Phone: 34-963983225; Fax: 34-963987860; E-mail: daniel.monleon@uv.es.

doi: 10.1158/0008-5472.CAN-10-1498

©2010 American Association for Cancer Research.

will improve these clinical decisions as well as patient follow-up strategy after surgery.

Metabolomics is defined as “the quantitative measurement of the multiparametric metabolic response of living systems to pathophysiological stimuli or genetic modification” (9). High-resolution nuclear magnetic resonance (NMR) spectroscopy of biofluids and tissues combined with multivariate analysis methodologies, such as principal component analysis (PCA), represent a powerful technique for investigating the metabolome in the area of drug toxicology and disease diagnosis and prognosis (10). NMR is one of the most efficient, robust, reproducible, and cheap methods for obtaining metabolic profiles in biological specimens without extensive sample preparation (11). High-resolution magic angle spinning (HR-MAS) NMR spectroscopy is a powerful technique for the investigation of metabolites within different intact tissues (12–16). The potential of HR-MAS applications to the study of biological tissues has been widely shown in the investigation of different cellular alterations. In addition, HR-MAS NMR spectroscopy of intact tissues (*ex vivo*) provides further advantages over traditional high-resolution liquid NMR of tissue extracts (*in vitro*). This technology can supplement histopathologic examination and potentially improve brain tumor diagnostics. HR-MAS spectra generate metabolic profiles that contain information on physiologic and pathologic status. This approach can be used to define the metabolomic phenotype of a tissue.

The aim of this study was to detect new subgroups of meningioma and to achieve higher specificity in the classification of meningioma by measuring metabolic phenotypes with high-resolution NMR spectroscopy. We collected HR-MAS spectra on 34 benign and 12 atypical meningioma tissue samples and used multivariate analysis for detecting metabolic subgroups. Histopathology after NMR, which is only possible when using HR-MAS methodologies, provides an essential validation of our results. This analysis shows that genetic instability has high effect on the metabolic profile of meningioma samples.

Materials and Methods

Patients and clinical samples

Forty-six human meningioma biopsies were obtained from 46 patients at the Department of Neurosurgery of the Clinical University Hospital of Valencia. This study was reviewed and approved by the local ethics committee. During surgery, most of the resected tissue was sent for routine histologic analysis, and the remainder was immediately put in cryogenic vials and snap frozen in liquid nitrogen. All snap-frozen samples were stored in a freezer at -80°C until further analysis. All samples used for histopathologic examination were fixed in neutral-buffered formalin, embedded in paraffin, sectioned, and stained with H&E. Tumors were classified according to the 2007 WHO histologic classification (2). Meningioma types analyzed include 34 benign meningiomas (grade 1) and 12 atypical meningiomas (grade 2).

Cytogenetic analysis and fluorescence *in situ* hybridization

Cytogenetic analyses were performed by short-term culture of the tumors. Fresh tumor samples were disaggregated with 2 mg/mL of collagenase II. The cells were seeded in flasks using RPMI 1640 supplemented with 20% fetal bovine serum, L-glutamine, and antibiotics. The cells were processed after 72 hours of culture by a standard technique. Air-dried slides were banded by trypsin-Giemsa. Karyotypic analyses were performed according to ISCN (17).

The samples of meningioma used for fluorescence *in situ* hybridization (FISH) analysis were studied by tissue microarrays. We removed four 0.6-mm cores from the corresponding areas on the paraffin block in each case using the Beecher Instruments Manual Tissue Arrayer I. For the investigation of chromosome abnormalities by interphase FISH, the probes LSI 22q12, LSI 1p36/LSI 1q25, and LSI t(11;14) IGH/CCND1 (Vysis, Inc.) were used.

Hybridizations were performed according to the instructions that accompany the probe. Counterstaining of nuclei was carried out using 4',6-diamidino-2-phenylindole. The fluorescent signal was detected using a photomicroscope Axioplan 2 and Axiophot 2 (Zeiss) equipped with a set of the appropriate filters. For each hybridization, green and orange signals were counted in the four regions of a total of 100 to 200 nonoverlapping nuclei. An interpretation of deletion or imbalance was made when >20% of the nuclei harbored these alterations (18, 19). Cutoffs for deletions were based on the frequencies of signals for the same probes in nonneoplastic brain controls (median, ± 3) and ranged from 14% to 21% for chromosome 1, from 16% to 22% for chromosome 14, and from 15% to 20% for monosome 22. We considered deletion when one or less signal for chromosome appeared with respect to the signal of control (ratio, 0/1, 0/2, 1/2, 1/3...), and we considered normal with the probes used present a ratio 2/2.

HR-MAS spectroscopy

Total sample preparation time for each sample before NMR detection was <5 minutes. All the material to be in contact with the tissue was precooled to reduce tissue degradation during the sample preparation process. Frozen samples were taken from the ultrafreezer and immediately placed in a cryovial and in liquid N_2 until insertion in a 4-mm outer diameter ZrO_2 rotor. The HR-MAS tissue sample was split from the whole frozen tumoral mass submerged in liquid nitrogen. The precooled rotor was filled with cooled D_2O after tissue sample insertion. Cylindrical inserts were used in all the cases, limiting the rotor inner volume to 50 μL . Exceeding D_2O was removed before rotor sealing. Tissue samples were weighted in the rotor before D_2O addition and HR-MAS measurements. Tissue fragments were weighted exclusively for sample preparation purposes. The mean sample weight was 27 ± 11 mg. Immediately after the measurement, the HR-MAS samples were fixed in formalin for subsequent histopathologic examination and for tumor content assessment by an expert pathologist.

All spectra were recorded in a Bruker Avance DRX 600 spectrometer operating at a ^1H frequency of 600.13 MHz.

The instrument was equipped with a 4-mm triple resonance $^1\text{H}/^{13}\text{C}/^{15}\text{N}$ HR-MAS probe with magnetic field gradients aligned with the magic angle axis. For all experiments, samples were spun at 5,000 Hz to keep the rotation sidebands out of the acquisition window. Lock homogeneity was achieved by extensive coil shimming using the one-dimensional water presaturation experiments in interactive mode as control. Alanine doublet at 1.475 ppm was used for lock homogeneity shimming, as described elsewhere (20). Nominal temperature of the sample receptacle was kept at 273 K using the cooling of the inlet gas pressures responsible for the sample spinning. This value corresponded to the temperature measured from the thermocouple just below the rotor in the probe. The effect of sample rotation was to slightly increase this value. Internal measurement using a 100% methanol sample in a 4-mm rotor spinning at the same frequency provided a corrected internal value of 277 K. To minimize the effects of tissue degradation, which would alter the metabolite composition of the biopsy, all *ex vivo* spectra were acquired at this temperature of 277 K. A total of 10 minutes was allowed for the temperature of the sample to reach steady state before spectra were acquired. A single-pulse presaturation experiment was acquired in all the samples. The number of transients was 256 collected into 32 K data points for all the experiments. Water presaturation was used during 1 second along the recycling delay for solvent signal suppression. Spectral widths were 8,000 Hz for 1 hour. Before Fourier transformation, the free induction decay was multiplied with a 0.3-Hz exponential line broadening. Chemical shift referencing was performed relative to the alanine CH_3 signal at 1.475 ppm. For assignment purposes, two-dimensional (2D) homonuclear (2D-TOCSY) and heteronuclear (2D- ^1H , ^{13}C -HSQC) experiments were acquired on selected samples.

NMR data analysis

All 30 spectra were processed using MNova 5.3 (Mestrelab S.A.) and transferred to MATLAB (MathWorks, Inc.) using in-house scripts for data analysis. All multivariate analysis was performed using the PLS_Toolbox library. The chemical shift region including resonances between 0.50 and 4.60 ppm and between 5.20 and 10.50 was investigated. For comparison of global metabolic profiles from different meningioma subgroups, the spectra were binned into 0.01 ppm buckets, normalized to total spectral integral, and subsequently analyzed by PCA. The spectral binning and normalization minimized the effect of differences in tissue weight and cell content for the different biopsies. We cross-validated our PCA model by performing 10 technical replicates by choosing random training (36 samples) and validation (10 samples) data subsets. Cross-validation is a technique for assessing how the results of a statistical analysis will generalize to an independent data set. The first two principal components of the average model (PC1 and PC2) accounted for a total of 65% of the variance in the spectral data set. Lower-order principal components did not provide clear differences between subgroups and consequently were not further analyzed. Spectral signal integration by peak-fitting algorithms over relevant resonances provided relative levels of the corresponding metabolites. Only those

signals with peak-fitting residual error lower than 10% were used in the study.

Statistical analysis

To determine individual metabolic differences between the different subgroups of meningioma, univariate Student's *t* tests were performed for each signal of the individual metabolites detected as major contributor in the PCA analysis. We calculated the maximum false discovery rate (FDR) of the metabolites selected to account for multiple testing. FDR was estimated using the *q* value statistical parameter (21). The *q* value gives the estimated FDR for every possible list of significant signals. The *q* value is based on estimating the true proportion of null hypotheses. The *P* value histogram width used for calculating *q* values was 0.005. Because we performed three comparisons and the *q* value may be different, the *q* value was applied separately to the *P* values of each comparison. Unless otherwise indicated, the limit of *q* value for metabolites selected in each comparison was set to 0.05 (FDR of 5%).

Results

Histopathology

Histologic analysis of the tissue specimens after HR-MAS analysis showed various amounts of tumor tissue (Fig. 1). In all cases, histologic analysis of the HR-MAS sample agreed with the histopathology original diagnosis. All samples included a percentage of tumor cells at least of 80%, as evaluated by two expert pathologists exploring at 10 \times the whole sample (1–2 mm), confirming that samples are representative of the tumor, independently of tumor grade.

Chromosomal profile

Karyotyping was obtained in 37 cell cultures from 37 different cases. Sample material was adequate for FISH studies in 42 cases. Information from both methodologies was combined to distinguish complex chromosomal profiles. Thirty-seven of 46 meningiomas presented clonal numerical and/or structural abnormalities, as shown in Table 1 and Supplementary Materials and Methods. All cases without chromosomal aberrations belonged to the histologic grade 1 meningioma group. Monosomy of chromosome 22 is the most common genetic alteration in meningioma and was detected in 22 of all cases. All cases without a complex karyotype were of histologic grade 1. Similarly, all those cases with alterations in chromosome 22 as the only chromosomal anomaly were also of histologic grade 1. According to FISH chromosomal analysis, only 16% (5 of 32) of benign meningiomas are $-1p$, whereas this percentage rises to 70% (7 of 10) in atypical meningioma. All cases containing alterations in chromosome 14 were of histologic grade 2. All grade 2 meningiomas showed a complex karyotype, with six of them showing chromosomal alterations different to $-1p$, -22 , and/or -14 . These findings confirm that exploration of chromosomes beyond 1, 14, and 22 is recommended for genetic characterization of meningiomas. Our results show that meningiomas with higher histologic grade (grade 2) are very

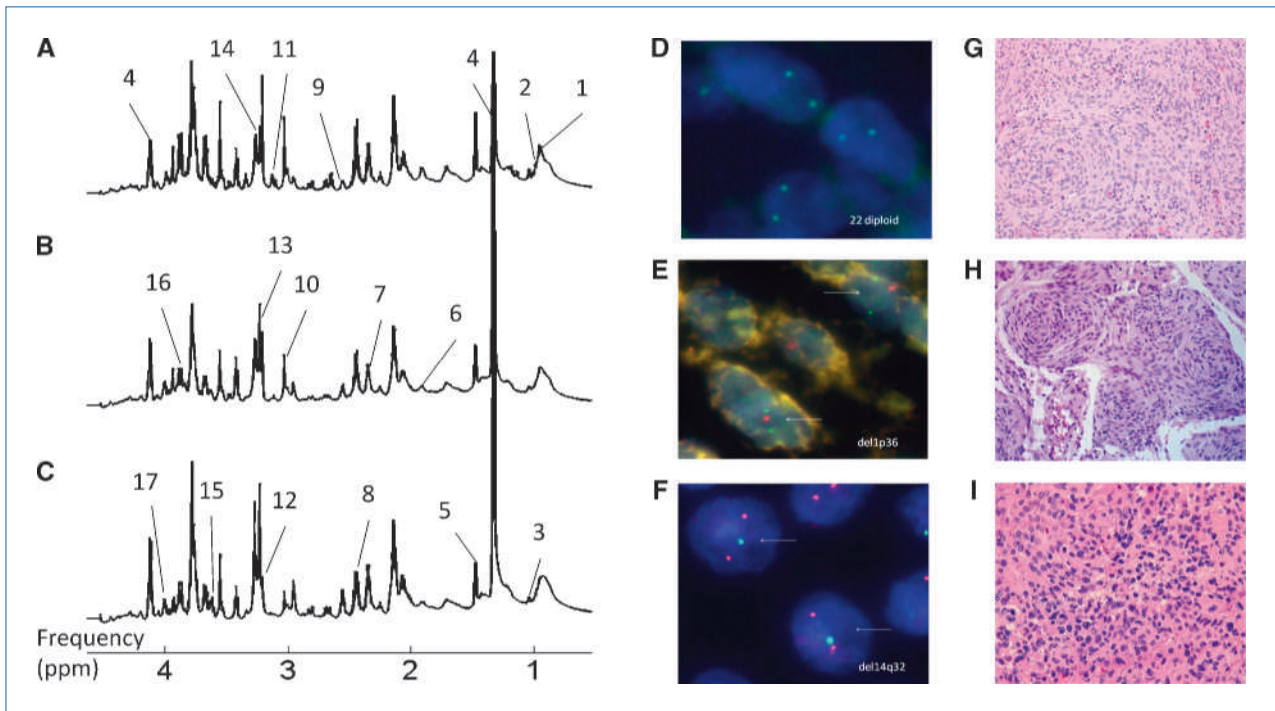


Figure 1. Representative NMR spectra (A–C), FISH images (D–F), and histopathology (G–I) for the benign meningioma without chromosomal instabilities (meningothelial meningioma, subgroup benignA; A, D, and G), benign meningioma with chromosomal instabilities (transitional meningioma, subgroup benignB; B, E, and H), and atypical meningioma (C, F, and I). Resonances belonging to metabolites with statistical significance have been labeled in the spectra (1, fatty acids; 2, leucine; 3, isoleucine; 4, lactate; 5, alanine; 6, acetate; 7, glutamate; 8, glutamine; 9, total glutathione; 10, creatine; 11, ethanolamine; 12, choline; 13, phosphocholine; 14, taurine; 15, glycine; 16, glucose; 17, phosphoethanolamine). FISH images show chromosomes 22 (D; normal), 1 (E; 1p deletion as red spots), and 14 (F; 14q deletion as green spots).

likely to have a complex karyotype. There is a subpopulation of meningiomas with histologic grade 1, which also exhibits complex karyotype, despite not having alterations in chromosome 14. Besides 1, 14, and 22, chromosomes affected either in this benign meningioma subgroup or in atypical meningioma include 2, 3, 5, 7, 9, 10, 17, and 18. Differently to some previous studies, the combined use of FISH and cytogenetics allowed the detection of many different anomalous chromosomal profiles. Based on chromosomal profiles, we defined three meningioma subgroups for subsequent

analysis: histologic grade 1 with normal or diploid karyotype (benignA), histologic grade 1 with complex karyotype (benignB), and histologic grade 2 (atypical).

Metabolic profile

HR-MAS spectroscopy provided well-resolved spectra of intact meningioma tissue samples. NMR spectra of benignA, benignB, and atypical meningioma are displayed in Fig. 1. The PCA analysis (Fig. 2) showed partial group separation between meningiomas benignA and meningiomas with

Table 1. Summary of chromosomal instabilities detected in benign and atypical meningioma according to cytogenetic and FISH analysis

	Chromosomal instabilities					Nonclonal [†]	FISH				Total
	Normal	-22	-1p	-14	Others*		-22q	-1p	-14q	Diploid	
BenignA	8	7	—	—	—	—	10	—	—	8	20
BenignB	—	9	3	—	13	5	9	5	—	3	14
Atypical	—	6	3	4	7	2	7	7	4	—	12

NOTE: Cells in gray show the chromosomal instability progression in the different subgroups of meningioma.

*Numerical or structural alterations different to monosomy 22, 1p deletion, and monosomy 14 (see Supplementary Materials and Methods).

[†]Numerical or structural alterations, which are present only once in the different metaphases analyzed.

complex karyotype (benignB and atypical). On the other hand, histologic benign and atypical meningiomas formed two partially overlapping groups. The overlapping region contained most of the meningioma tumors showing chromosomal instabilities, indicating metabolic similarity between benign meningiomas with chromosomal instabilities (benignB subgroup) and the more aggressive atypical meningioma tumors. In the next step, individual metabolites were identified in the PCA loading plot and quantified for further analysis. A total of 19 metabolites showed statistically significant differences between either two of the three subgroups (Table 1). No statistically significant correlation was detected between FISH quantitative data (see Supplementary Materials and Methods) and the metabolic profiles (Table 2).

The major features for separation between benignA meningioma and atypical meningioma (the two subgroups clearly separated in the PCA scores plot) were higher concentrations of glycine, glutamate, total glutathione, lactate, taurine, phosphocholine, phosphoethanolamine, and uracil and lower concentrations of global fatty acids, γ -aminobutyric acid, ascorbate, acetate, creatine, alanine, leucine, isoleucine, glutamine, ascorbate, lysine, glucose, choline, and ethanolamine. For most of these metabolites, with the exception of taurine, glutamine, and γ -aminobutyric acid, the values for benignB meningioma were closer to atypical meningioma than to benignA meningioma (Table 1; Fig. 3). Meningioma with complex karyotype showed increased levels of glutamate and total glutathione and reduced levels of glutamine, suggesting an increase in total glutathione production. Glucose, ascorbate, acetate, and fatty acids (metabolites involved in the tricarboxylic acid cycle) and fatty acid β -oxidation were all decreased in the same groups. Conversely, lactate was higher in atypical meningioma. Increased glucose uptake and high glycolytic activity, due to high energy requirement, are major hallmarks of tumor metabolism. These changes usually result in decreased intracellular glucose concentrations and higher levels of lactate. However, these metabolites

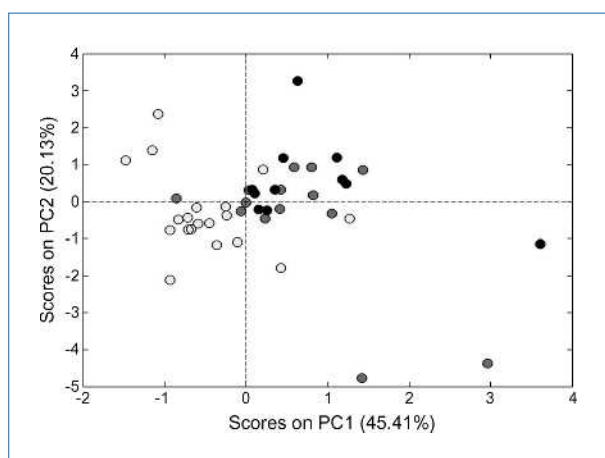


Figure 2. Score plots of PCA to compare the metabonome of the benign meningioma without chromosomal instabilities (subgroup benignA, white circles), the benign meningioma with chromosomal instabilities (subgroup benignB, gray circles), and the atypical meningioma (black circles).

may also be altered by the biopsy extraction procedure. Phosphocholine and phosphoethanolamine, both phospholipid derivatives, also showed increased levels in meningioma groups with complex karyotype. Increased membrane metabolite turnover is another significant metabolic pathway for tumor development and aggressiveness. On the other hand, the similar levels of polyunsaturated and monounsaturated fatty acids in all groups suggested a similar amount of necrotic fraction in the tissue. Finally, despite high variability, uracil metabolites increased with complex karyotype progressively and in a statistically significant manner. This suggests that nucleotide metabolism is also altered in more aggressive tumors.

Discussion

Most meningiomas are classified as benign based on clinical and pathologic findings. Nonetheless, the behavior of individual meningioma is still difficult to predict. Many previous studies report some correlation between chromosomal alterations and meningioma clinical outcome. Typically, these correlations are usually weak because of two reasons. First, the chromosomal profile typically is limited to FISH analysis of a few chromosomes. Second, clinical outcome takes years to be properly assessed and still many individuals may exhibit the clinical aggressiveness later on. Maillo and colleagues (22) show that statistical correlation between genetic abnormalities and clinical outcome improves when follow-up is extended to 10 years, with a subset of patients showing recurrence 15 years after surgery. On the other hand, most of the previously reported meningioma subgroups define aggressiveness based solely on WHO grade and morphologic parameters. This definition of the phenotype of an aggressive meningioma is rather poor. The metabolic changes of any cell population precede morphologic changes. In fact, chromosomal alterations produce changes in the metabolic phenotype almost immediately. The measurement of a metabolic phenotype at the moment of the histopathologic diagnosis may help in detecting better defined molecular meningioma subgroups.

In our study, chromosomal profiling by cytogenetics and FISH and metabolic profiling by NMR spectroscopy on benign and atypical meningioma reveal distinct molecular phenotypes that allowed detecting metabolic aggressiveness in these tumors. Previous studies on metabolic profiling of meningiomas report weak correlations between grade and metabolic phenotype (19, 23). This may be due to the use of tissue extracts, which precludes the histopathology of the sample and makes impossible to know the tumor content, leading to much broader variability in the metabolite levels. To our knowledge, this is the first combined genetic and metabolic analysis of intact biopsies of benign and atypical meningiomas for detecting metabolic subgroups. The use of cytogenetics allows the detection of a global chromosomal profile. Similarly, NMR spectroscopy combined with multivariate analysis provides a global metabolic profile. The combination of these data provides a robust and well-delimited set of meningioma subgroups.

Table 2. Resonance intensity ratios, SDs, and *P* values from most relevant metabolites in the classification of benign and atypical meningiomas

Metabolite (peak position)	Relative intensity (arbitrary units)			<i>P</i>		
	BenignA	BenignB	Atypical	BenignA vs BenignB	BenignA vs atypical	BenignB vs atypical
Fatty acids (0.89 ppm)	73 ± 24	45 ± 18	52 ± 21	0.008	0.016	0.388
Leucine (0.97 ppm)	45 ± 15	30 ± 10	34 ± 12	0.019	0.072	0.333
Isoleucine (1.02 ppm)	28 ± 7	20 ± 6	23 ± 7	0.008	0.011	0.141
Lactate (1.33 ppm)	211 ± 121	302 ± 99	341 ± 132	0.028	0.008	0.401
Alanine (1.48 ppm)	58 ± 24	29 ± 18	31 ± 17	0.001	0.002	0.797
Acetate (1.92 ppm)	21 ± 8	16 ± 8	15 ± 7	0.078	0.032	0.662
Glutamate (2.35 ppm)	23 ± 4	27 ± 7	31 ± 8	0.014	0.265	0.037
Glutamine (2.44 ppm)	30 ± 9	30 ± 18	23 ± 5	0.978	0.059	0.256
Total glutathione (2.55 ppm)	12 ± 6	17 ± 4	17 ± 8	0.081	0.009	0.913
Creatine (3.03 ppm)	48 ± 22	29 ± 17	25 ± 13	0.011	0.004	0.595
Ethanolamine (3.15 ppm)	10 ± 3	8 ± 3	7 ± 3	0.051	0.012	0.150
Choline (3.19 ppm)	43 ± 12	30 ± 12	29 ± 15	0.012	0.011	0.731
Phosphocholine (3.22 ppm)*	61 ± 35	82 ± 28	91 ± 40	0.077	0.043	0.551
Taurine (3.26 ppm)	25 ± 8	26 ± 8	32 ± 9	0.745	0.025	0.064
Glycine (3.55 ppm)	26 ± 8	30 ± 7	34 ± 9	0.361	0.030	0.167
Glucose (3.88 ppm)	41 ± 17	36 ± 14	28 ± 11	0.317	0.011	0.095
Phosphoethanolamine (4.01 ppm)	14 ± 7	15 ± 6	23 ± 9	0.839	0.008	0.008
Ascorbate (4.52 ppm)†	2 ± 1	—	—	—	—	—
Uracil (7.54 ppm)†	—	2 ± 1	2 ± 1	—	—	0.983

NOTE: Most of the metabolites show values for BenignB meningioma closer to atypical than to BenignA meningioma, suggesting metabolic aggressiveness in this subgroup.

**q* > 0.05.

†Signal intensity was not sufficient for quantification in all the samples.

Chromosomal aberrations in a tumor sample are typically studied by FISH. FISH is a target-oriented method that allows direct observation of specific chromosomal abnormalities. It is more sensitive than standard cytogenetic methods because it does not require dividing cells and can be measured directly in the tumor tissue. However, cytogenetic methods provide a whole-genome chromosomal profiling and may reveal chromosomal alterations in regions different to those explored by target-oriented methods. The combination of both methods provides a global chromosomal profile with high sensitivity in specific regions. Therefore, we found chromosomal alterations that would not have been detected by any of the individual approaches alone. We chose to examine chromosomes 1, 14, and 22 by FISH because aberrations of those chromosomes are the most frequently reported genetic abnormalities in meningioma (7). Our findings confirmed that loss of 1p and/or 14 are the most common chromosomal alterations in atypical meningioma. Coexistence of monosomy 14 and 1p is a powerful adverse prognostic factor for early relapses (6). However, meningiomas are cytogenetically heterogeneous tumors. The detection of a subset of benign meningiomas with chromosomal alterations beyond monosomy 22 may have an important effect in defining aggressiveness in meningiomas. This subset of benign meningiomas

(benignB subgroup) shows a wide variety of chromosomal alterations, all producing a complex karyotype. Histologic benign meningiomas with complex karyotype have higher probability of relapsing (22). In line with this, in the present study, all histologic benign meningiomas with complex karyotype (subgroup benignB) show a metabolic phenotype similar to that of atypical meningioma.

The metabolic phenotype of meningiomas with complex karyotype shows typical features of aggressive tumor biochemistry such as increased membrane metabolite turnover and high glycolytic activity. Lower levels of glucose and ascorbate together with higher levels of lactate suggest higher dependence on anaerobic breakdown of pyruvate for meningiomas with complex karyotype. Lactate accumulation also creates a microenvironment that may enhance cell proliferation (24). Lower glucose levels in cells of more aggressive tumors may reflect preferential glucose consumption and a local hypoxic microenvironment. Hypoxia in the tumor microenvironment triggers a variety of genetic and adaptive responses that regulate tumor growth (25). Tumor hypoxia is often associated with more malignant phenotypes, resistance to therapy, and poor survival. Another metabolite closely related to energy metabolism is creatine. Total creatine is lower in meningiomas with chromosomal instabilities. This

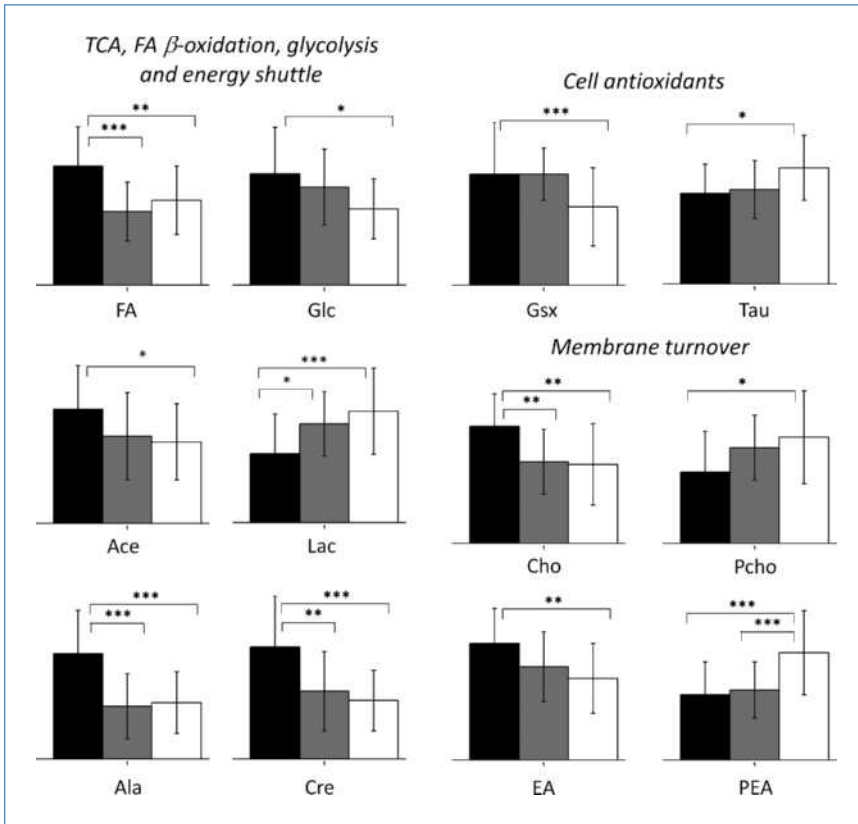


Figure 3. Histograms showing relevant metabolite levels, SD error bars, and significance levels (*, $P < 0.05$; **, $P < 0.02$; ***, $P < 0.01$) for the benign meningioma without chromosomal instabilities (subgroup benignA, black columns), the benign meningioma with chromosomal instabilities (subgroup benignB, gray columns), and the atypical meningioma (white columns). FA, fatty acids; Glc, glucose; Ace, acetate; Lac, lactate; Ala, alanine; Cre, creatine; Gsx, total glutathione; Tau, taurine; Cho, choline; EA, ethanolamine; PCho, phosphocholine; PEA, phosphoethanolamine.

may indicate either lower substrate availability or increased ATP usage, which suggests an environment with high energy demand. Finally, the decreased levels of fatty acids may also reflect increased β -oxidation. All these processes result in a metabolically unfavorable microenvironment with low glucose availability and local hypoxic conditions. Our results suggest that meningiomas with chromosomal instabilities have this energy-demanding microenvironment.

Choline-containing compounds are elevated in tumors (26, 27). Phosphocholine and choline compounds are gener-

ally considered as well-established proliferation markers. In addition, high phosphocholine is also correlated with highly invasive phenotypes. However, these compounds are not easily detected by conventional high-resolution NMR. The tissue extraction process disables the direct observation of small cellular proteins and membrane semimobile phospholipids precursors. On the contrary, HR-MAS allows the determination of these important metabolites in intact biopsies. Meningiomas with chromosomal instabilities have higher phosphocholine levels, which are consistent with higher

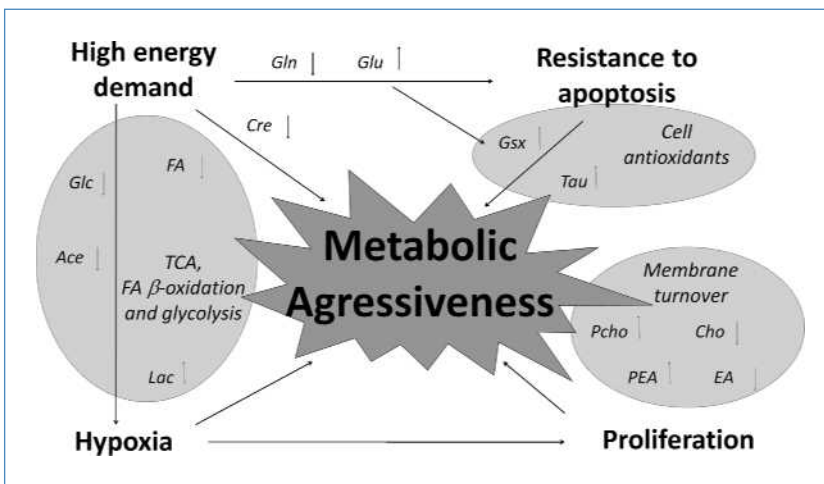


Figure 4. Scheme showing the interconnection between the different metabolites and processes involved in the metabolic aggressiveness observed for the benign meningioma with chromosomal instabilities. Essentially, the metabolic differences observed in benign meningioma with chromosomal instabilities with respect to other benign meningioma suggest higher energy demand and metabolic activity, higher proliferation rates, higher antioxidant capacity, and higher hypoxia, which are indicative of more aggressive tumors.

proliferative rates. In addition, phosphoethanolamine, which is also considered as an intermediate in the metabolism of phospholipids, exhibits increased levels in meningioma with chromosomal instabilities. A high relative intensity of the phosphoethanolamine resonance in ^{31}P MR spectroscopy is a reported marker for malignancy (28). Increased phosphoethanolamine levels suggest an activation of phosphatidylethanolamine metabolism, which is involved in the modification of membrane shape in malignant tissue (29). Additionally, free phosphoethanolamine might reflect the breakdown of phosphatidylethanolamine to diacylglycerol, and might act as a long-term second messenger for cell proliferation (30).

Glutathione is an important cell antioxidant and, in normal tissues, plays different roles in protection against oxidative damage (31), in apoptosis (32–34), and in amino acid transport (35). Glutathione depletion is a common feature of apoptotic cell death. In cancer, glutathione is able to play both protective and pathogenic roles (31). In addition, there is a correlation between decreased total glutathione levels and cell differentiation. In meningioma, levels of glutathione and closely related metabolites, such as glutamate, are increased with respect to other brain tumors and healthy brain tissue (36). A potential explanation for this is the reversible transamination reaction of alanine and α -ketoglutarate, synthesizing glutamate, as an alternative energy source. This may also explain the lower levels of alanine in atypical meningioma despite higher hypoxic conditions. Another source of glutamate is glutamine by the glutaminase reaction, which also explains the lower levels found for glutamine in the same subgroup. Meningioma with chromosomal instabilities shows increased levels of glutathione and glutamate and decreased levels of alanine and glutamine, which suggest less cell differentiation, resistance to apoptosis, and activation of alternative energy sources.

The aforementioned metabolites and pathways play critical roles in cancer metabolism. All of them suggest that meningiomas with chromosomal instabilities suffer metabolic alterations related to aggressiveness, proliferation, and invasiveness (see Fig. 4 for a schematic view). Other metabolic changes reported here are also in the same line. For example, glycine, which is the simplest nonessential amino acid and is associated to recurrence in some brain tumors (37), is in-

creased in meningioma with complex karyotype. Glycine is a major component of collagen. Increased levels of glycine suggest increased collagen synthesis and artery wall formation, and therefore sustained angiogenesis. Increased levels of uracil in meningioma with chromosomal instabilities may reflect the activation of uracil glycosylase, which excises uracil from DNA deaminated cytosine and repairs damaged DNA. Previous studies reported that uracil glycosylase activity correlates with tumor recurrence (38).

In summary, the metabolic phenotype detected by HR-MAS in meningioma allows detecting metabolic aggressiveness in histologic benign tumors. The multivariate analysis shows that benign meningioma with complex karyotype (benignB subgroup) is metabolically closer to atypical meningioma than to other benign meningiomas (benignA subgroup). Most of the metabolites showing statistically significant differences between groups suggest a more aggressive biochemistry in meningiomas with chromosomal instabilities regardless of their histologic grade. To our knowledge, this is the first time that distinct metabolic phenotypes are reported for otherwise benign meningiomas based on cytogenetic studies and multivariate analysis and global metabolic profiling of intact tumor biopsies. Overall, this work shows that the measurement of a metabolic phenotype in meningioma intact biopsies simultaneously to the histopathology analysis may allow the early detection of metabolically aggressive tumors.

Disclosure of Potential Conflicts of Interest

No potential conflicts of interest were disclosed.

Grant Support

Conselleria de Sanidad (GV-AP064/07, GV-AP076/08, and GV-AP014/09) and the Conselleria de Educaci3n (ACOMP2009-200) de la Generalitat Valenciana, the Ministerio de Educaci3n y Ciencia del Gobierno de Espa1a (SAF2008-00270). D. Monle3n gratefully acknowledges the Ministerio de Educaci3n y Ciencia del Gobierno de Espa1a for a Ramon y Cajal 2006 Contract.

The costs of publication of this article were defrayed in part by the payment of page charges. This article must therefore be hereby marked *advertisement* in accordance with 18 U.S.C. Section 1734 solely to indicate this fact.

Received 04/28/2010; revised 09/14/2010; accepted 09/14/2010; published OnlineFirst 09/21/2010.

References

- Perry A, Scheithauer BW, Stafford SL, Lohse CM, Wollan PC. "Malignancy" in meningiomas: a clinicopathologic study of 116 patients, with grading implications. *Cancer* 1999;85:2046–56.
- Louis DN, Ohgaki H, Wiestler OD, et al. The 2007 WHO classification of tumours of the central nervous system. *Acta Neuropathol* 2007; 114:97–109.
- McLendon RE, Rosenblum MK, Bigner DD, editors. Russell & Rubinstein's pathology of tumours of the central nervous system. 7th ed. London: Hodder Arnold; 2006.
- Dumanski JP, Rouleau GA, Nordenskjold M, Collins VP. Molecular genetic analysis of chromosome 22 in 81 cases of meningioma. *Cancer Res* 1990;50:5863–7.
- Pfisterer WK, Hank NC, Preul MC, et al. Diagnostic and prognostic significance of genetic regional heterogeneity in meningiomas. *Neuro-oncol* 2004;6:290–9.
- Lopez-Gines C, Cerda-Nicolas M, Gil-Benso R, et al. Association of loss of 1p and alterations of chromosome 14 in meningioma progression. *Cancer Genet Cytogenet* 2004;148:123–8.
- Perry A, Gutmann DH, Reifenberger G. Molecular pathogenesis of meningiomas. *J Neurooncol* 2004;70:183–202.
- Pfisterer WK, Coons SW, Aboul-Enein F, Hendricks WP, Scheck AC, Preul MC. Implicating chromosomal aberrations with meningioma growth and recurrence: results from FISH and MIB-I analysis of grades I and II meningioma tissue. *J Neurooncol* 2008;87:43–50.
- Nicholson JK, Lindon JC. Systems biology: metabolomics. *Nature* 2008;455:1054–6.
- Nicholson JK, Connelly J, Lindon JC, Holmes E. Metabolomics: a platform for studying drug toxicity and gene function. *Nat Rev Drug Discov* 2002;1:153–61.
- Serkova NJ, Spratlin JL, Eckhardt SG. NMR-based metabolomics: translational application and treatment of cancer. *Curr Opin Mol Ther* 2007;9:572–85.

12. Sitter B, Sonnewald U, Spraul M, Fjosne HE, Gribbestad IS. High-resolution magic angle spinning MRS of breast cancer tissue. *NMR Biomed* 2002;15:327–37.
13. Monleón D, Morales JM, Gonzalez-Darder J, et al. Benign and atypical meningioma metabolic signatures by high-resolution magic-angle spinning molecular profiling. *J Proteome Res* 2008;7:2882–8.
14. Cheng LL, Wu C, Smith MR, Gonzalez RG. Non-destructive quantitation of spermine in human prostate tissue samples using HRMAS 1H NMR spectroscopy at 9.4 T. *FEBS Lett* 2001;494:112–6.
15. Cheng LL, Ma MJ, Becerra L, et al. Quantitative neuropathology by high resolution magic angle spinning proton magnetic resonance spectroscopy. *Proc Natl Acad Sci U S A* 1997;94:6408–13.
16. Cheng LL, Chang IW, Louis DN, Gonzalez RG. Correlation of high-resolution magic angle spinning proton magnetic resonance spectroscopy with histopathology of intact human brain tumor specimens. *Cancer Res* 1998;58:1825–32.
17. Mitelman F, editor. *ISCN 1995: an international system for human cytogenetic nomenclature*. Basel (Switzerland): Karger Publishers, Inc.; 2009.
18. Ambros PF, Ambros IM. Pathology and biology guidelines for resectable and unresectable neuroblastic tumors and bone marrow examination guidelines. *Med Pediatr Oncol* 2001;37:492–504.
19. Pfisterer WK, Hendricks WP, Scheck AC, et al. Fluorescent *in situ* hybridization and *ex vivo* 1H magnetic resonance spectroscopic examinations of meningioma tumor tissue: is it possible to identify a clinically-aggressive subset of benign meningiomas? *Neurosurgery* 2007;61:1048–59, discussion 60–1.
20. Piotto M, Elbayed K, Wieruszkeski JM, Lippens G. Practical aspects of shimming a high resolution magic angle spinning probe. *J Magn Reson* 2005;173:84–9.
21. Storey JD, Tibshirani R. Statistical significance for genomewide studies. *Proc Natl Acad Sci U S A* 2003;100:9440–5.
22. Maillo A, Orfao A, Espinosa AB, et al. Early recurrences in histologically benign/grade I meningiomas are associated with large tumors and coexistence of monosomy 14 and del(1p36) in the ancestral tumor cell clone. *Neuro Oncol* 2007;9:438–46.
23. Pfisterer WK, Nieman RA, Scheck AC, Coons SW, Spetzler RF, Preul MC. Using *ex vivo* proton magnetic resonance spectroscopy to reveal associations between biochemical and biological features of meningiomas. *Neurosurg Focus* 2010;28:E12.
24. Brahimi-Horn MC, Chiche J, Pouyssegur J. Hypoxia signalling controls metabolic demand. *Curr Opin Cell Biol* 2007;19:223–9.
25. Brahimi-Horn MC, Chiche J, Pouyssegur J. Hypoxia and cancer. *J Mol Med* 2007;85:1301–7.
26. Glunde K, Jacobs MA, Bhujwala ZM. Choline metabolism in cancer: implications for diagnosis and therapy. *Expert Rev Mol Diagn* 2006;6:821–9.
27. Glunde K, Jie C, Bhujwala ZM. Molecular causes of the aberrant choline phospholipid metabolism in breast cancer. *Cancer Res* 2004;64:4270–6.
28. Kinoshita Y, Yokota A, Koga Y. Phosphorylethanolamine content of human brain tumors. *Neurol Med Chir (Tokyo)* 1994;34:803–6.
29. Cullis PR, Hope MJ, Tilcock CP. Lipid polymorphism and the roles of lipids in membranes. *Chem Phys Lipids* 1986;40:127–44.
30. Radda GK, Dixon RM, Wood CA. N.m.r. studies of phospholipid metabolism and cell proliferation. *Biochem Soc Trans* 1991;19:995–6.
31. Balendiran GK, Dabur R, Fraser D. The role of glutathione in cancer. *Cell Biochem Funct* 2004;22:343–52.
32. Filomeni G, Aquilano K, Rotilio G, Ciriolo MR. Glutathione-related systems and modulation of extracellular signal-regulated kinases are involved in the resistance of AGS adenocarcinoma gastric cells to diallyl disulfide-induced apoptosis. *Cancer Res* 2005;65:11735–42.
33. Locigno R, Castronovo V. Reduced glutathione system: role in cancer development, prevention and treatment (review). *Int J Oncol* 2001;19:221–36.
34. Esteve JM, Mompo J, Garcia de la Asuncion J, et al. Oxidative damage to mitochondrial DNA and glutathione oxidation in apoptosis: studies *in vivo* and *in vitro*. *FASEB J* 1999;13:1055–64.
35. Orłowski M. Possible role of glutathione in transport processes. *Adv Exp Med Biol* 1976;69:13–28.
36. Opstad KS, Provencher SW, Bell BA, Griffiths JR, Howe FA. Detection of elevated glutathione in meningiomas by quantitative *in vivo* 1H MRS. *Magn Reson Med* 2003;49:632–7.
37. Lehnhardt FG, Rohn G, Ernestus RI, Grune M, Hoehn M. ¹H- and ³¹P-MR spectroscopy of primary and recurrent human brain tumors *in vitro*: malignancy-characteristic profiles of water soluble and lipophilic spectral components. *NMR Biomed* 2001;14:307–17.
38. Moon YW, Park WS, Vortmeyer AO, et al. Mutation of the uracil DNA glycosylase gene detected in glioblastoma. *Mutat Res* 1998;421:191–6.